

# Stiffness of Asphalt Concrete Surface Layer from Stress Wave Measurements

MARWAN F. AOUAD, KENNETH H. STOKOE II, AND ROBERT C. BRIGGS

The spectral analysis of surface waves (SASW) method is an in situ seismic technique used to evaluate the stiffness of the asphalt concrete (AC) surface layer as well as the stiffnesses of lower layers in a pavement profile. Measurements are made at low strain levels; hence testing is nondestructive. A key element in performing SASW measurements is the generation and detection of surface waves. To sample the AC surface layer, wavelengths less than the surface layer thickness need to be generated. This requirement can only be accomplished with sources generating high frequencies (frequencies generally above 20 kHz). Two high-frequency sources, a small hammer and a piezoelectric generator, were used. Results show that the piezoelectric generator performed better than the small hammer as a high-frequency source, especially for temperatures above 80°F. SASW measurements made at the pavement test facility in Bryan, Texas, indicated how it is possible to quantify changes in the stiffness of the AC surface layer with ambient temperature changes. These in situ measurements along with similar measurements made on Route 1 in Austin, Texas, show how Young's modulus,  $E$ , of the AC surface layer changes with temperature in the manner predicted by the AASHTO guide for temperatures below 100°F. However, for temperatures above 100°F, the AASHTO guide overpredicts the decrease in  $E$  with increasing temperatures based on the in situ SASW results. In the case of thin AC surface layers, layers with a thickness on the order of 1 in. (2.5 cm) or less, wavelengths shorter than the thickness of the surface layer could not be generated so that the surface layer could not be evaluated with SASW tests. In such cases, compressional stress wave measurements are suggested.

The spectral analysis of surface waves (SASW) method is a nondestructive and nonintrusive method for evaluating stiffness profiles of pavement systems using stress (seismic) waves. General application of the SASW method to pavement systems can involve extensive testing and analytical modeling. However, the method is readily applied to measurements of surface layers when the layer thickness is on the order of several inches. This application is demonstrated herein by tests performed on AC surface layers at the Texas Transportation Institute (TTI) Annex in Bryan, Texas, and on Route 1 in Austin, Texas. The effectiveness of the test in determining in situ changes in AC surface layer stiffness due to changes in ambient temperature is shown, and limitations of the method on thin AC surface layers are noted.

SASW testing was performed at three sites at the TTI facility [Sites 4, 9, and 12 as designated by Scrivner and Michalak (1)]. These sites have AC surface layers that are about 5 in. (12.5 cm) in thickness. Such surface layers are considered

"thick" layers in the context of SASW testing. Each site was tested at two different seasons of the year. The first series of tests involved measurements in the summer (during the last week of July 1988) when the temperature of the surface layer ranged from 80°F to 143°F. The second series involved measurements during the cold season, in the first week of March 1989, when the temperature ranged from 30°F to 81°F. SASW tests were also performed at Sites 10 and 11 at the TTI facility, which have an AC layer thickness of 1 in. (2.5 cm). These sites are considered to have a "thin" surface layer in the context of SASW testing. In this case, compressional wave testing was also performed during the cold season of the year to evaluate the stiffness of the surface layer.

A suite of SASW and compressional wave tests was also performed on the AC surface layer of Route 1 in Austin, Texas. This pavement is composed of a thick surface layer, which was tested within 1.5 years after placement, in contrast with the AC surface layers at TTI, which are about 25 years old.

The objectives of testing at TTI and Route 1 were to study the effects of temperature, thickness, and age of the AC layer on the measurement of stiffness, to determine whether the SASW method ceases to perform adequately at some surface layer thicknesses, to recommend when other techniques (such as compression wave testing) should be used in place of the SASW method to characterize the AC surface layer, and to evaluate the importance of frequency in these measurements. Stiffness variations of AC with temperature and frequency are dependent on asphalt type. This variable was not studied because the thrust of this work dealt with developing the methodology needed to apply SASW and compression wave testing to AC surface layers.

## SASW METHOD

The SASW method was initiated at the University of Texas at Austin in the early 1980s with funding from The Texas State Department of Highways and Public Transportation (2-4). Key elements in the SASW technique are the generation and detection of surface waves using a source and two receivers placed on the pavement surface. Two strengths of the SASW method are (a) all measurements are made from the pavement surface and (b) a pavement stiffness profile in terms of Young's modulus can be obtained without knowing the layer thicknesses. These two strengths make the SASW method effective in testing pavement systems where the pavement surface layer is intact. In addition, research has been conducted at several universities during the last decade to

M. F. Aouad and K. H. Stokoe II, Department of Civil Engineering, The University of Texas at Austin, Austin, Tex. R. C. Briggs, Texas Department of Transportation, Austin, Tex.

improve the theoretical and practical aspects of the method (5-11).

When SASW measurements are performed, a source and two receivers are placed on the pavement surface such that the distance from the source to the first receiver is equal to the distance between the two receivers. A dynamic signal analyzer is used to capture and process the receiver outputs denoted by  $x(t)$  and  $y(t)$  for Receivers 1 and 2, respectively. Then  $x(t)$  and  $y(t)$  are transformed to the frequency domain [ $X(f)$  and  $Y(f)$ ] through the use of a Fast Fourier Transform.  $X(f)$  and  $Y(f)$  are used to calculate the cross power spectrum between the two receivers, denoted by  $G_{XY}$  [ $G_{XY} = X(f) \cdot Y(f)$ , where \* denotes the complex conjugate]. The surface wave velocity and wavelength as a function of frequency,  $V_R(f)$  and  $\lambda(f)$ , are determined from these results by

$$\Theta_{XY}(f) = \tan^{-1} [\text{Im}(G_{XY})/\text{Re}(G_{XY})] \quad (1)$$

$$t(f) = \Theta_{XY}(f)/(360^\circ \cdot f) \quad (2)$$

$$V_R(f) = D/t(f) \quad (3)$$

$$\lambda(f) = V_R(f)/f \quad (4)$$

where

$\Theta_{XY}(f)$  = phase shift of the cross power spectrum in degrees at each frequency,

Im = imaginary part of the cross power spectrum at each frequency,

Re = real part of the cross power spectrum at each frequency,

$f$  = frequency,

$t(f)$  = time delay between receivers as a function of frequency, and

$D$  = distance between receivers.

In addition, values of a coherence function are calculated in these measurements. The coherence function,  $\gamma^2(f)$ , is defined as

$$\gamma^2(f) = |G_{XY}|^2/(G_{XX} \cdot G_{YY}) \quad (5)$$

where

$\|$  = magnitude of the cross power spectrum,

$G_{XX}$  = power spectrum of Receiver 1, and

$G_{YY}$  = power spectrum of Receiver 2.

The coherence will be equal to unity where the input and output signals are correlated (noise free). Typical functions for  $\Theta_{XY}$  and  $\gamma^2$  are shown in Figure 1 for receivers spaced 6 in. (15.2 cm) apart.

In an elastic, isotropic medium, the elastic constants are determined from the surface wave velocity according to the following relationships:

$$V_S = C \cdot V_R \quad (6)$$

$$G = (\gamma/g) \cdot V_S^2 \quad (7)$$

$$E = 2G(1 + \nu) \quad (8)$$

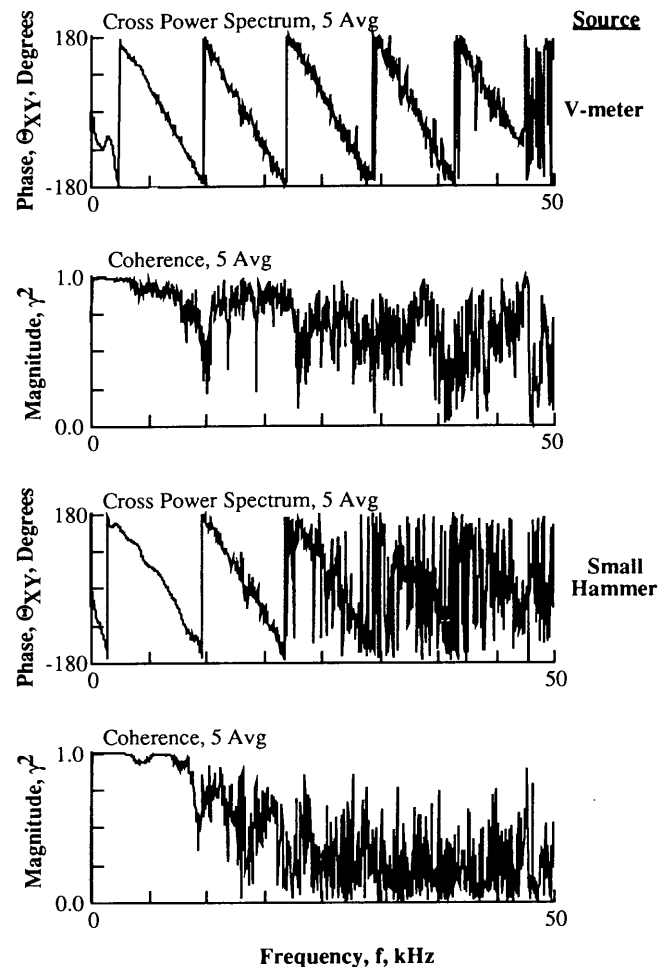


FIGURE 1 Comparison of phases of the cross power spectra and coherence functions using two sources, Site 12 at TTI Annex ( $T = 97^\circ\text{F}$ , receiver spacing = 6 in., AC thickness  $\approx$  5 in.).

where

$V_S$  = shear wave velocity,

$C = 1.135 - 0.182 \cdot \nu$  (for  $\nu \geq 0.1$ ),

$G$  = shear modulus,

$\gamma$  = total unit weight,

$g$  = acceleration of gravity,

$E$  = Young's modulus, and

$\nu$  = Poisson's ratio.

A Poisson's ratio of 0.27 was assumed unless compression wave measurements were made.

#### SASW MEASUREMENTS AT SITES 4, 9, AND 12

The asphalt concrete pavement stiffness ( $E$ ) is dependent on temperature and frequency because of the viscous nature of asphalt. The modulus of the pavement can change significantly with temperature and frequency. To quantify in-place changes in  $E$  of the AC layer with temperature, SASW tests were performed at Sites 4, 9, and 12 at the TTI Annex.

The first series of tests was conducted during July 1988 when the surface temperature varied from 80°F in the morning (5:30 a.m.) to about 143°F in the afternoon (2:15 p.m.). Two sources were used. A small ball-peen hammer [weight about 2 oz (57 gm)] and a V-meter (piezoelectric source with central output frequency of 54 kHz) were compared as high-frequency generators. The surface waves were monitored with two PCB Model 308B02 accelerometers placed on the pavement surface. The accelerometers have a resonant frequency of 25 kHz and a calibration factor of 1 V/g. The accelerometers were coupled to the asphalt concrete by attaching 10-32 threaded rods to the bottom of the accelerometers, which, in turn, were attached to 10-32 nuts glued to the AC surface. This approach was used so that exactly the same points could always be tested.

The small hammer and V-meter were evaluated to determine whether they could provide the high frequencies required to evaluate the AC layer. A comparison of the cross power spectra and coherence functions [ $\Theta_{XY}(f)$  and  $\gamma^2(f)$  in Equations 1 and 5] from SASW measurements at Site 12 using both sources is shown in Figure 1. The V-meter generated energy up to 45 kHz, as opposed to the maximum 20-kHz energy generated by the small hammer as noted in the cross power spectra. Despite the poor coherence at frequencies above 20 kHz due to attenuation and background noise interference, the cross power spectrum using the V-meter as a source could be easily interpreted to obtain the experimental dispersion curve. As the temperature of the surface layer rose, the surface layer became too soft to allow impact sources such as the small hammer to be used as a high-frequency source. On the basis of this comparison, the V-meter was adopted as the better source for the generation of high frequencies and was used for the remainder of the first test series.

The second series of SASW tests was conducted during March 1989, when the surface temperature varied from 30°F early in the morning (5:50 a.m.) to 81°F in the early afternoon (12:45 p.m.). The source used to generate the high frequencies in the second series of tests was the small ball-peen hammer because of its simplicity. The performance of this source was checked against the V-meter for low surface temperatures. A comparison of the cross power spectra and coherence functions at Site 12 using both sources is shown in Figure 2. The small hammer performed well over the range of temperatures and frequencies required to sample the surface layer. Both sources generated energy up to 50 kHz. The generated surface waves were detected by two WR (Wilcoxon Research) Model 736 accelerometers placed on the pavement surface. These accelerometers have a resonant frequency above 50 kHz and a calibration factor of 0.1 V/g. The accelerometers were coupled to the asphalt concrete by attaching a magnet to a steel plate at the bottom of the accelerometers, which, in turn, was attached to a nail driven into the surface layer. This coupling method was faster and more convenient than the approach used in the first series of tests and represents the method of choice.

A comparison of the phases of the cross power spectra for a temperature range from 30°F to 143°F using the V-meter as a source and a receiver spacing of 6 in. (15.2 cm) at Site 12 is shown in Figure 3. This comparison shows the deterioration of the phase shift of the cross power spectrum as the surface

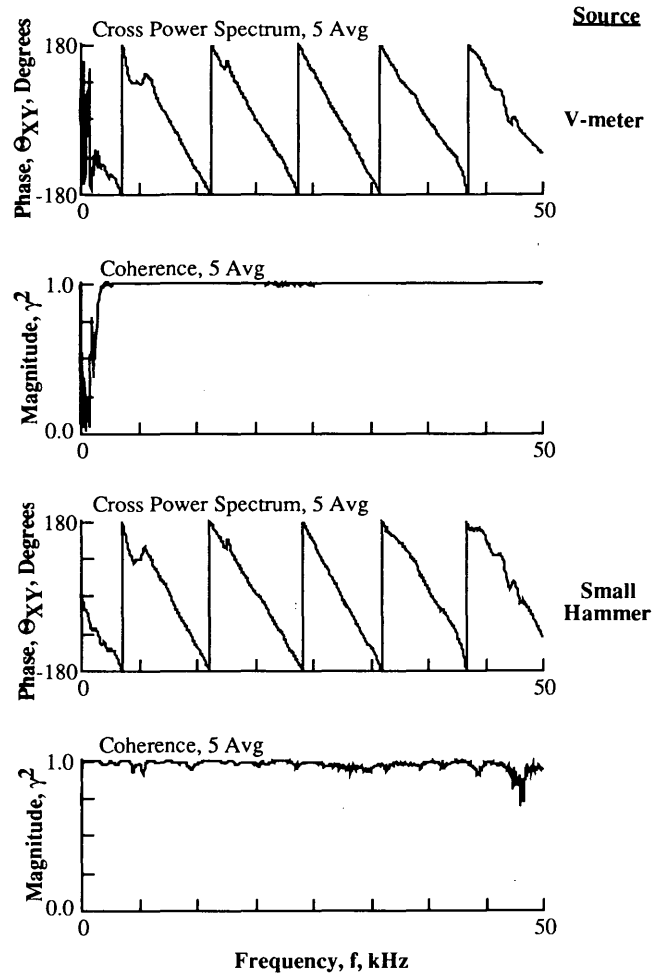
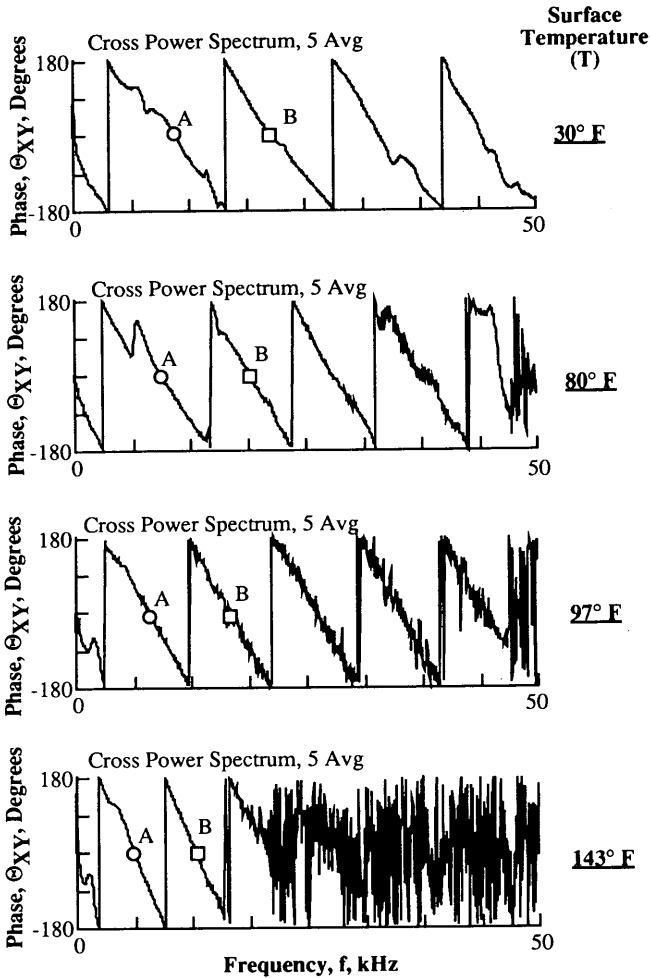


FIGURE 2 Comparison of phases of the cross power spectra and coherence functions using two sources, Site 12 at TTI Annex ( $T = 59^\circ\text{F}$ , receiver spacing = 6 in., AC thickness  $\approx$  5 in.).

layer warms. At a temperature of 30°F, frequencies up to 50 kHz were generated, as opposed to frequencies of about 18 kHz when the temperature rose to 143°F. The same behavior was observed at Sites 4 and 9.

**Experimental Dispersion Curves**

The phase shifts of the cross power spectra and the coherence functions were used to obtain the experimental dispersion curves shown in Figures 4a and 4b for Sites 4 and 12, respectively. The dispersion curves for Site 9 were similar to those for Site 12. The experimental dispersion curves shown are the composite dispersion curves based on receiver spacings of 0.5 and 1 ft (0.15 and 0.3 m). The 1-ft (0.3-m) spacing was used to sample the base layer. However, that measurement was used only slightly in these tests. To illustrate how the measured phase shifts,  $\Theta_{XY}$ 's, are used to calculate wave velocities, consider Points A and B on each curve in Figure 4b. These points are shown in the field measurements in Figure 3. Point A corresponds to a surface wave velocity and wave-



Note: Points A and B shown in dispersion curves in Fig. 4b

**FIGURE 3** Variation in phase of the cross power spectrum as the asphalt concrete surface layer warms from 30°F to 143°F, Site 12 at TTI Annex (V-meter source, receiver spacing = 6 in., AC thickness ≈ 5 in.).

length calculated from Equations 1 through 4 for a phase shift of 360 degrees between receivers. This phase shift gives different wave velocities for different temperatures because the frequency at which the 360°-degree phase shift occurred decreased as temperature increased. Point B corresponds to a surface wave velocity and wavelength for a phase shift of 720 degrees between receivers.

Figures 4a and 4b indicate that the stiffness of the surface layer can be determined with great precision as it warms or cools. This value is simply calculated from the average of all values of  $V_R$  at wavelengths shorter than the layer thickness [6 in. (15.2 cm) in this case]. At a temperature of 30°F, an average value of the surface wave velocity of the asphalt layer was found to be 5,430 fps (1655 m/sec) as opposed to the value of 3,370 fps (1025 m/sec) at a temperature of 143°F. These values correspond to Young's moduli of 2,735 ksi ( $18.8 \times 10^3$  MPa) and 1,055 ksi ( $7.3 \times 10^3$  MPa) at 30°F and 143°F, respectively. These values of  $E$  correspond to an average measurement frequency of 15 kHz and, thus, must be corrected for frequency for use in design or for comparison with

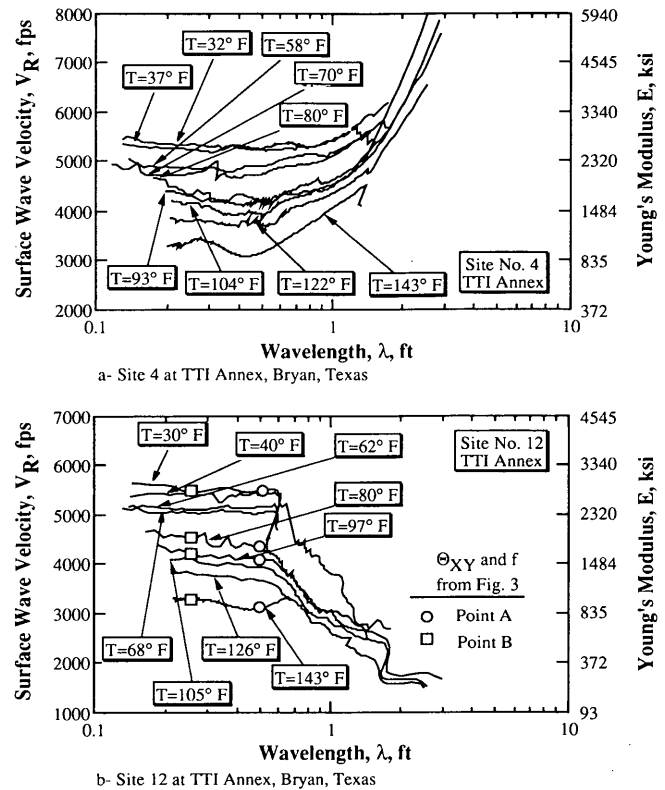


**FIGURE 4** Change in stiffness of the asphalt concrete surface layer (thickness ≈ 5 in.) as a result of solar heating or cooling.

results from other tests such as the falling weight deflectometer (say at about 30 Hz). The SASW-determined moduli values should, therefore, be divided by the correction factor shown in Figure 5. The solid data points in Figure 5 represent extrapolated values from curves obtained by Sousa and Monismith (12). Additional testing has been conducted by the first author in the laboratory with field cores (13), and these results are shown by the open symbols. The solid curve represents a potential frequency correction curve to adjust high-frequency SAW measurements to those at a frequency of 30 Hz.

Figure 4 also indicates a slight decrease in velocity with increasing wavelength in the surface layer, suggesting a frequency dependence of the stiffness of the AC layer (most

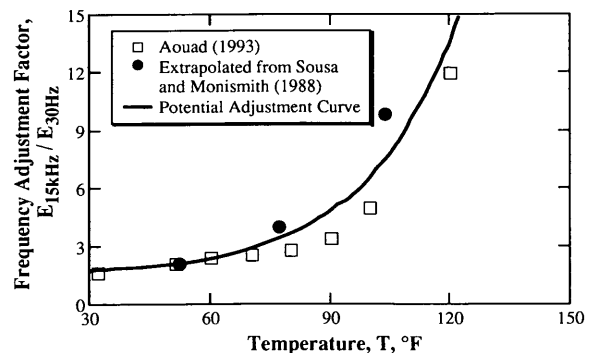


**FIGURE 5** Variation of frequency adjustment factor with temperature for asphalt concrete.

easily seen in Figure 4b above temperatures of 68°F). Finally, the base material was sampled with SASW measurements using a 1-ft (0.3-m) receiver spacing. Without any further analysis of the data, it is clear that the base material of Site 4, which consists of 4 percent cement-stabilized crushed limestone, is stiffer than the surface layer because the surface wave velocity increases as wavelength increases above 0.55 ft (0.17 m) (Figure 4a). On the other hand, surface wave velocity decreases at wavelengths greater than 0.55 ft (0.17 m) at Site 12, indicating a softer material below the surface layer. This is further shown in Figure 6, which shows a comparison of the dispersion curves of Sites 4 and 12 for measurements at two different temperatures. From the SASW measurements, the thickness of the surface layer was determined to be about 0.55 ft (0.17 m), which is in reasonable agreement with the thickness of 0.42 ft (0.13 m) shown on the construction drawings. The layer thickness was determined as equaling the wavelength at which the surface wave velocities begin to change from the nearly constant value representing the surface layer (14).

**Adjustment of Modulus for Frequency**

Values of surface wave velocities determined from the SASW measurements were used to calculate Young's moduli of the surface layer using Equations 6 through 8. A unit weight of 140 pcf (22 kN/m<sup>3</sup>) and a Poisson's ratio of 0.27 were assumed for the AC layer. Table 1 gives surface wave velocities and Young's moduli for wavelengths of 0.25 and 0.42 ft (0.08 and 0.13 m). The wavelength of 0.25 ft (0.08 m) was selected because it was the minimum wavelength measured when the surface temperature rose to 143°F. The wavelength of 0.42 ft (0.13 m) was selected because it corresponds to the as-built thickness of the AC surface layer. Figure 7 shows the variation of the surface layer modulus with temperature. At a wavelength of 0.25 ft (0.08 m), the modulus exhibits a slightly higher value than at a wavelength of 0.42 ft (0.13 m), primarily because of the effect of frequency.

As an initial attempt to remove the effect of frequency, the moduli of the surface layer were calculated using surface wave velocities at a frequency of 15 kHz and were normalized to a modulus at 70°F [ $E_{70°F} \approx 2,140$  ksi ( $14.8 \times 10^3$  MPa)]. The

**TABLE 1 Surface Wave Velocities and Young's Moduli of the Asphalt Concrete Surface Layer at Wavelengths of 0.25 and 0.42 ft Determined from SASW Measurements at Sites 4, 9, and 12**

| Temp (°F) | Site 4              |         |                     |         | Site 9              |         |                     |         | Site 12             |         |                     |         |
|-----------|---------------------|---------|---------------------|---------|---------------------|---------|---------------------|---------|---------------------|---------|---------------------|---------|
|           | $\lambda = 0.25$ ft |         | $\lambda = 0.42$ ft |         | $\lambda = 0.25$ ft |         | $\lambda = 0.42$ ft |         | $\lambda = 0.25$ ft |         | $\lambda = 0.42$ ft |         |
|           | $V_R$ (fps)         | E (ksi) | $V_R$ (fps)         | E (ksi) | $V_R$ (fps)         | E (ksi) | $V_R$ (fps)         | E (ksi) | $V_R$ (fps)         | E (ksi) | $V_R$ (fps)         | E (ksi) |
| 30        | -----               | -----   | -----               | -----   | -----               | -----   | -----               | -----   | -----               | -----   | -----               | -----   |
| 32        | 5359                | 2665    | 5249                | 2557    | -----               | -----   | -----               | -----   | -----               | -----   | -----               | -----   |
| 37        | 5251                | 2559    | 5190                | 2500    | -----               | -----   | -----               | -----   | -----               | -----   | -----               | -----   |
| 40        | -----               | -----   | -----               | -----   | -----               | -----   | -----               | -----   | 5246                | 2553    | 5195                | 2504    |
| 43        | -----               | -----   | -----               | -----   | 5292                | 2598    | 5190                | 2499    | -----               | -----   | -----               | -----   |
| 56        | -----               | -----   | -----               | -----   | 5098                | 2411    | 5010                | 2329    | -----               | -----   | -----               | -----   |
| 58        | 4878                | 2208    | 4920                | 2246    | -----               | -----   | -----               | -----   | -----               | -----   | -----               | -----   |
| 62        | -----               | -----   | -----               | -----   | -----               | -----   | -----               | -----   | 5146                | 2457    | 5142                | 2453    |
| 68        | -----               | -----   | -----               | -----   | -----               | -----   | -----               | -----   | 5036                | 2353    | 5034                | 2351    |
| 70        | 4811                | 2148    | 4737                | 2082    | -----               | -----   | -----               | -----   | -----               | -----   | -----               | -----   |
| 72        | -----               | -----   | -----               | -----   | 4782                | 2122    | 4736                | 2081    | -----               | -----   | -----               | -----   |
| 80        | 4368                | 1770    | 4216                | 1649    | -----               | -----   | -----               | -----   | 4484                | 1865    | 4286                | 1704    |
| 81        | -----               | -----   | -----               | -----   | 4495                | 1874    | 4191                | 1629    | -----               | -----   | -----               | -----   |
| 89        | -----               | -----   | -----               | -----   | 4433                | 1823    | 4170                | 1613    | -----               | -----   | -----               | -----   |
| 93        | 4326                | 1736    | 4199                | 1636    | -----               | -----   | -----               | -----   | -----               | -----   | -----               | -----   |
| 97        | -----               | -----   | -----               | -----   | -----               | -----   | -----               | -----   | 4193                | 1631    | 4090                | 1552    |
| 104       | 4171                | 1614    | 3937                | 1438    | 3984                | 1472    | 3822                | 1355    | -----               | -----   | -----               | -----   |
| 105       | -----               | -----   | -----               | -----   | -----               | -----   | -----               | -----   | 4120                | 1575    | 3917                | 1423    |
| 117       | -----               | -----   | -----               | -----   | 3870                | 1389    | 3770                | 1318    | -----               | -----   | -----               | -----   |
| 122       | 3821                | 1354    | 3729                | 1290    | -----               | -----   | -----               | -----   | -----               | -----   | -----               | -----   |
| 126       | -----               | -----   | -----               | -----   | -----               | -----   | -----               | -----   | 3828                | 1359    | 3648                | 1234    |
| 139       | -----               | -----   | -----               | -----   | 3436                | 1095    | 3330                | 1029    | -----               | -----   | -----               | -----   |
| 143       | 3417                | 1083    | 3193                | 946     | -----               | -----   | -----               | -----   | 3272                | 993     | 3105                | 894     |

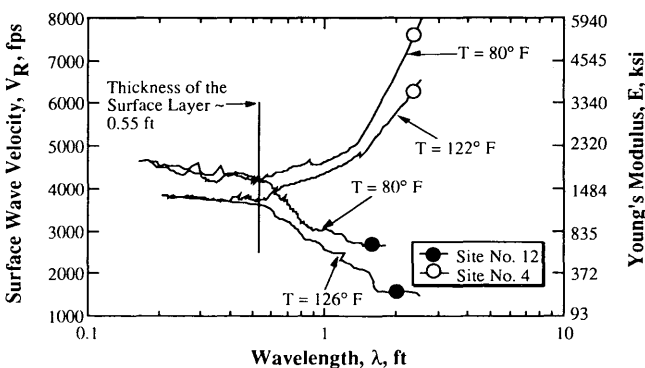


**FIGURE 6 Comparison of experimental dispersion curves determined at Sites 4 and 12 for two temperatures.**

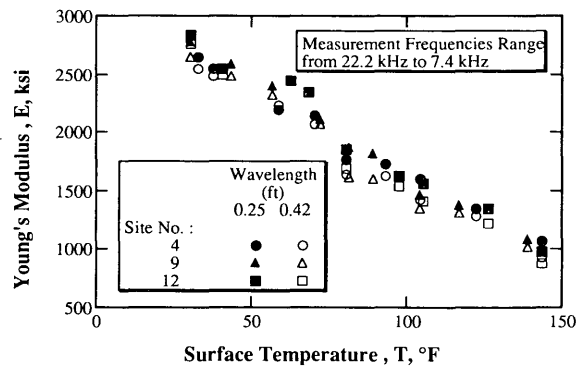


**FIGURE 7 Variation in low-strain Young's modulus with temperature for wavelengths of 0.25 and 0.42 ft at the TTI Annex, Bryan, Texas.**

frequency of 15 kHz was selected because it was about the highest frequency generated when the temperature rose to 143°F. Table 2 gives the surface wave velocities and normalized moduli at a frequency of 15 kHz. The variation of normalized modulus with temperature is presented in Figure 8. A change in modulus by a factor of about 2.6 was observed for the change in temperature from 30°F to 143°F. When such correlation curves become well established, thin pavements, which are especially difficult to test at high temperatures as discussed in the next section, could be tested when cool, and

**TABLE 2 Surface Wave Velocities and Normalized Young's Moduli of the Asphalt Concrete Surface Layer Determined from SASW Measurements at Sites 4, 9, and 12; Measurement Frequency  $\approx$  15 kHz**

| Site 4    |                         |                     | Site 9    |                         |                     | Site 12   |                         |                     |
|-----------|-------------------------|---------------------|-----------|-------------------------|---------------------|-----------|-------------------------|---------------------|
| T<br>(°F) | V <sub>R</sub><br>(fps) | E/E <sub>70°F</sub> | T<br>(°F) | V <sub>R</sub><br>(fps) | E/E <sub>70°F</sub> | T<br>(°F) | V <sub>R</sub><br>(fps) | E/E <sub>70°F</sub> |
| 32        | 5316                    | 1.2266              | 30        | 5431                    | 1.2802              | 30        | 5545                    | 1.3345              |
| 37        | 5254                    | 1.1981              | 43        | 5250                    | 1.1963              | 40        | 5246                    | 1.1945              |
| 58        | 4880                    | 1.0336              | 56        | 5081                    | 1.1205              | 62        | 5146                    | 1.1494              |
| 70        | 4800                    | 1.0000              | 72        | 4817                    | 1.0071              | 68        | 5063                    | 1.1126              |
| 80        | 4400                    | 0.8403              | 81        | 4440                    | 0.8556              | 80        | 4474                    | 0.8688              |
| 93        | 4223                    | 0.7740              | 89        | 4380                    | 0.8327              | 97        | 4160                    | 0.7511              |
| 104       | 4100                    | 0.7296              | 104       | 3984                    | 0.6889              | 105       | 4050                    | 0.7119              |
| 122       | 3821                    | 0.6337              | 117       | 3870                    | 0.6500              | 126       | 3800                    | 0.6267              |
| 143       | 3378                    | 0.4953              | 139       | 3440                    | 0.5136              | 143       | 3291                    | 0.4701              |

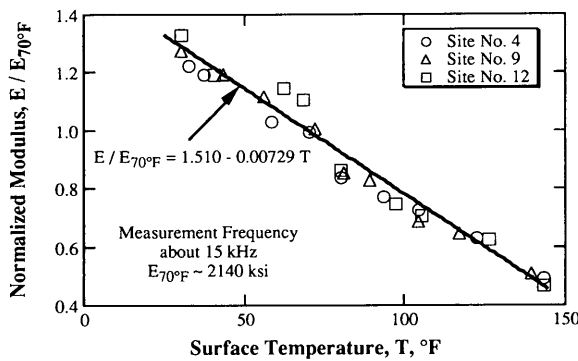


**FIGURE 8 Variation in normalized low-strain Young's modulus (normalized to a modulus at a temperature of 70°F) with temperature for three sites at the TTI Annex, Bryan, Texas.**

values of moduli at higher temperatures could be obtained from correlation curves such as the one in Figure 8.

Normalized moduli of the asphalt concrete layer obtained from SASW measurements and corrected to a frequency of 30 Hz are shown in Figure 9. These corrected values are compared with values suggested by the *AASHTO Guide for Design of Pavement Structures* (15) in Figure 10. Figure 10

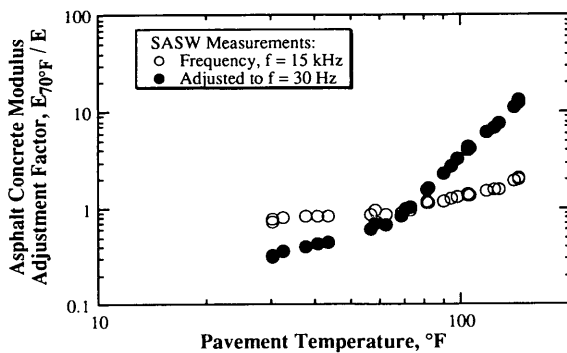


**FIGURE 9 Normalized modulus determined from SASW measurements at the TTI Pavement Facility and adjusted for frequency using Figure 5.**

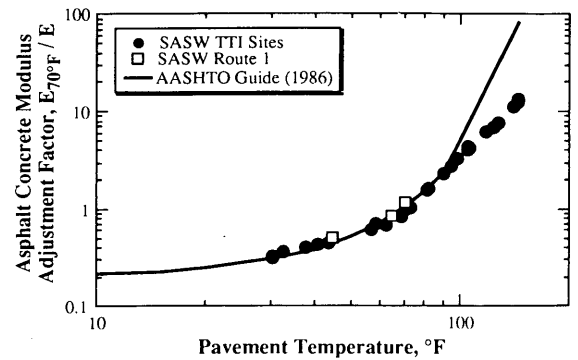


**FIGURE 10 Comparison of the variation of AC modulus with temperature from SASW measurements with that suggested by the *AASHTO Guide for Design of Pavement Structures* (15).**

indicates that the normalized moduli of the surface layer determined by SASW measurements at temperatures less than 100°F compare closely with normalized moduli suggested by the AASHTO guide. However, at temperatures above 100°F, in situ moduli determined by SASW testing are underestimated using the AASHTO guide. The SASW measurements were made at small strains (less than 0.001 percent). It is assumed that the lower values of moduli determined at high temperatures for the AASHTO guide are due to the higher strains associated with stress-controlled laboratory testing of soft AC specimens. At high temperatures, the behavior of asphalt is quite strain dependent. In addition, to accommodate the frequency effect in the SASW test, different adjustment factors are applied at different surface temperatures, as shown in Figure 5. The factor at high temperatures is large, and small errors in this factor could also contribute to the differences seen in Figure 10.

SASW tests similar to those performed at the TTI Annex were also performed on Route 1 in Austin, Texas. Testing was performed during February 1991, approximately 1.5 years after the AC layer 7 in. (17.8 cm) thick was placed. Results similar to those shown in Figures 3, 4b, and 8 were obtained. At a temperature of 70°F, an average value of the surface wave velocity of the AC layer was 5,410 fps (1650 m/sec). This value corresponds to a Young's modulus of 2,715 ksi ( $18.7 \times 10^3$  MPa), representing a stiffer AC layer than that encountered at the TTI facility, where  $E_{70°F} \approx 2,140$  ksi ( $14.8 \times 10^3$  MPa). Normalized moduli of the AC surface layer obtained from SASW measurements on Route 1 and corrected to a frequency of 30 Hz at temperatures of 70°F, 63°F, and 43°F are shown in Figure 10. The normalized values agree well with the curve suggested by the AASHTO guide at these temperatures.

**TESTING OF THIN ( $t \approx 1$  in.) AC SURFACE LAYERS**

Sites 10 and 11 at the TTI Annex were selected as representative pavement with thin AC surface layers. These sites consist of an AC layer 1 in. (2.5 cm) thick underlain by crushed limestone base and subbase. SASW measurements were performed at the two sites to evaluate the material profiles at

temperatures ranging from 70°F to 110°F. The stiffness of the surface layer could not be determined from the SASW measurements because wavelengths less than the thickness of the surface layer could not be generated. Therefore, no zone of short wavelengths, essentially constant velocities, was determined. The generation of short wavelengths was limited by the maximum aggregate size and the relatively high surface temperature. In this case, compression wave measurements should be performed in conjunction with the SASW measurements to determine the stiffness of the AC surface layer as discussed elsewhere (13).

## CONCLUSIONS

The SASW method was used at the TTI pavement facility in Bryan, Texas, and on Route 1 in Austin, Texas, to evaluate the stiffness of AC surface layers under different climatic conditions. The method proved to be effective in determining in situ changes in stiffness ( $E$ ) over temperatures ranging from 30°F to 143°F. The method was most effective at sites where the thickness of the surface layer was greater than 2 in. (5 cm) (referred to as "thick" surface layers herein). Young's moduli measured by the SASW tests represent high-frequency values and should be adjusted for frequency using Figure 5. The adjusted in situ moduli change with temperature in the same manner as predicted by the AASHTO guide (15) for temperatures below 100°F but show less sensitivity at temperatures above 100°F.

An essential element when performing SASW measurements to evaluate the stiffness of the AC surface layer is the generation of high frequencies, frequencies generally above 10 kHz. Two sources, a small hammer and a piezoelectric generator, were used, and the performance of each source was evaluated. The piezoelectric generator performed better than the small hammer as a high-frequency source, especially for temperatures of the AC surface layer above 80°F.

The SASW method was also used to determine the stiffness profiles of pavement sites where a "thin" AC surface layer was encountered [AC layer thickness  $\approx$  1 in. (2.5 cm)]. The stiffness of the AC surface layer could not be determined from SASW measurements because wavelengths shorter than 1 in. (2.5 cm) could not be generated. In such cases, direct compression wave measurements are suggested for use in characterizing the stiffness of the surface layer.

## ACKNOWLEDGMENTS

This work was supported by the Texas Department of Transportation. The authors wish to express their appreciation for this support.

## REFERENCES

1. F. Scrivner and C. H. Michalak. *Linear Elastic Layered Theory as a Model of Displacements Measured Within and Beneath Flexible Pavement Structures Loaded by the Dynaflect*. Research Report 123-25. Texas Transportation Institute, Texas A&M University, College Station, 1974.
2. J. S. Heisey, K. H. Stokoe II, W. R. Hudson, and A. H. Meyer. *Determination of In Situ Shear Wave Velocities from Spectral Analysis of Surface Waves*. Research Report 256-2. Center for Transportation Research, The University of Texas at Austin, Austin, 1982.
3. J. S. Heisey, K. H. Stokoe II, and A. H. Meyer. Moduli of Pavement Systems from Spectral Analysis of Surface Waves. In *Transportation Research Record 852*, TRB, National Research Council, Washington, D.C., 1982, pp. 22-31.
4. S. Nazarian. *In Situ Determination of Elastic Moduli of Soil Deposits and Pavement Systems by Spectral-Analysis-of-Surface-Waves Method*. Ph.D. dissertation. The University of Texas at Austin, Austin, 1984.
5. S. Nazarian and K. H. Stokoe II. *In Situ Determination of Elastic Moduli of Pavement Systems by Spectral-Analysis-of-Surface-Waves Method (Practical Aspects)*. Research Report 368-1F. Center for Transportation Research, The University of Texas at Austin, Austin, 1985.
6. S. Nazarian and K. H. Stokoe II. *In Situ Determination of Elastic Moduli of Pavement Systems by Spectral-Analysis-of-Surface-Waves Method (Theoretical Aspects)*. Research Report 437-2. Center for Transportation Research, The University of Texas at Austin, Austin, 1986.
7. J. C. Sheu. *Applications and Limitations of the Spectral-Analysis-of-Surface-Waves Method*. Ph.D. dissertation. The University of Texas at Austin, Austin, 1987.
8. I. Sánchez-Salineró. *Analytical Investigation of Seismic Methods Used for Engineering Applications*. Ph.D. dissertation. The University of Texas at Austin, Austin, 1987.
9. G. J. Rix. *Experimental Study of Factors Affecting the Spectral-Analysis-of-Surface-Waves Method*. Ph.D. dissertation. The University of Texas at Austin, Austin, 1988.
10. D. R. Hiltunen and R. D. Woods. Influence of Source and Receiver Geometry on the Testing of Pavements by the Surface Waves Method. In *Nondestructive Testing of Pavement and Back-calculation of Moduli*, STP 1026 (A. J. Bush III and G. Y. Baladi, eds.), ASTM, Philadelphia, Pa., 1989, pp. 138-154.
11. D. R. Hiltunen and R. D. Woods. Variables Affecting the Testing of Pavements by the Surface Waves Method. In *Transportation Research Record 1260*, TRB, National Research Council, Washington, D.C., 1990, pp. 42-52.
12. J. B. Sousa and C. L. Monismith. Dynamic Response of Paving Materials. In *Transportation Research Record 1136*, TRB, National Research Council, Washington, D.C., 1988, pp. 57-68.
13. M. F. Aouad. *Evaluation of Flexible Pavements and Subgrades Using the Spectral-Analysis-of-Surface-Waves (SASW) Method*. Ph.D. dissertation. The University of Texas at Austin, Austin, 1993 (in progress).
14. J. M. Roesset, D. W. Chang, K. H. Stokoe II, and M. F. Aouad. Modulus and Thickness of the Pavement Surface Layer from SASW Tests. In *Transportation Research Record 1260*, TRB, National Research Council, Washington, D.C., 1990, pp. 53-63.
15. Temperature-Deflection Corrections for Asphalt Pavements. Appendix L. *AASHTO Guide for Design of Pavement Structures*, AASHTO, Washington, D.C., 1986.